We are grateful for the constructive comments from our reviewers. We have made all the necessary comments (blue) to the reviewers queries *(italics)* and made the necessary changes to our manuscript (red). A strikeout through a reference refers to a figure, table or equation in the original manuscript.

Comment 1 - anonymous reviewer

My main concern is that the work is a somewhat incremental addition to the literature. It relies extensively on the publication by Ragazzola et al. 2012, both with regard to the data and the general concept. While an expansion to more complex models is valuable, it largely reflects the findings of the 2 vs. 3D structural FE analyses from other fields as cited in the text.

Ragazzola et al (2012)'s work was highly innovative, however these 2D models were simplistic in their very nature, and the results were not ground truthed against more complex natural geometries. The paper we present here represents novel work because it incorporates three-dimensional geometric models of coralline algae but, importantly, presents for the first time an FE-model of coralline algae derived from µCT data. To our knowledge this is one of the most complex computational models of a marine calcifier. Our results dont entirely reflect the findings of the 2D model. They show that: 1) a 2D model, such as Ragazzola et al. (2012) cannot accurately represent the mechanical performance of a 3D biological structure; 2) a 3D geometric model (constructed appropriately) can be used to accurately represent the mechanical performance of a biological structure; 3) future climate change may have significant impact on the mechanical performance of these organisms and 4) by verifying the use of simplified models, we can look at species specific changes and tailor our models easily, and accordingly, requiring less user and computing time and power. In response to further reviewers comments, we have performed additional analysis on our models (Page 4), which will add another feature to this paper independent of Ragazzola et al. (2012)'s work.

Page 5 line 91
These highly innovative models however were simplistic in nature. Importantly, they had not been tested to assess if they were a fair representation of skeletal mechanical performance. Consequently, the simple 2D model may have overestimated the distribution and magnitude of stress and hence future vulnerability of algal communities. Here we have developed a set of 3D FE geometric models to represent different aspects of coralline algae morphology and compared these models with a more biologically accurate 3D FE-model generated from computed tomography (CT) data, allowing us to assess the trade-off between computing time (Andersen and Jones, 2006; Romeed et al., 2006) and the need for an appropriate representation of the structure.

Page 15 line 286
As responses to climate change are species-specific, we are therefore able to create models tailor made to individual species and analyse how they react to future climate change.

I found the discussion of the factors not accounted for in the model quite useful (e.g. Mg content, proteins), but to have a larger impact on the readership of BGD, it would be helpful and necessary to expand on the environmental context of these simulations further. E.g., are the changes simulated environmentally significant? How does the load tested relate to typical stresses experienced in situ?

The loads applied to our models were estimated by Ragazzola et al. (2012). Further work (outside the scope of this paper) is required to analyse the nature of loads experienced in situ. We present a first attempt at this here, in additional models with revised loading conditions (see response to reviewer 2).

Page 5 line 86
Although the changes in growth rate were not significant, specimens grown under CO2 conditions predicted for the year 2050 were found to have significantly larger cells and thinner cell walls. These ultrastructure changes resulted in predicted increased vulnerability to fracture compared to present day structures ~~(Fig. 2a-b)~~ as observed in the 2D FE-model.

Page 8 Line 154
In keeping with Ragazzola et al. (2012), a load pressure of 20,000Pa was applied to the top left corner, 40 µm along the external top surface and 40 µm down the left surface of the models. Constraints were applied to the whole bottom surface and on the right hand surface, opposite the loads, 40 µm up from the constrained bottom. This simulated the attachment of the structure to the rest of the thallus ~~(Fig. 4)~~. Even though the same loads as Ragazzola et al. (2012) were used, it is known that the primary hydrodynamic force exerted on marine macroalgae is drag force (Carrington, 1990). Drag (Fdrag) force can be calculated using equation 1.

$$F_{drag} = 1/2(\rho U^2 A C_d) \quad (1)$$

Where ρ is the seawater density (approximately 1025 $\mathrm{kg\,m^{-3}}$); and U is water velocity. Subtidal marine macroalgae experience a water velocity on the order of magnitude of 1 $\mathrm{m\,s^{-1}}$ (Carrington, 1990), while intertidal species can experience breaking waves of up to 25 $\mathrm{m\,s^{-1}}$ (Denny et al., 2003). A is the algal planform area; and C_d the drag coefficient (dimensionless index of shape change and reconfiguration of flexible fronds (Carrington, 1990; Dudgeon and Johnson, 1992; Gaylord et al., 1994)). However, there are no data published for resulting in breakage of rhodoliths. The existing literature focused on flexible macroalgae, making it difficult to find loads that are environmentally significant whilst also being species related.

I am not convinced that statements such as we have confirmed previous results that future climate change will lead to a loss in the structural integrity of coralline algae are justified. Yes, the simulations here match the trends of published simulations, though the effect of increasing CO2 is much less, in particular for the strain energy.

We agree with the reviewer that this may be an overstatement, and hence the wording has been changed. See below for our change in manuscript.

Page 15, line 281
Using these more biologically accurate models, we have further supported previous results that state future climate change will lead to a loss in the structural integrity of coralline algae.

But more importantly, there is no validation of simulation results of actual structural damage with field data, and it is not obvious that effects from other adaptations can be ruled out completely.

In regards to validation of simulation results, there is currently no published experimental data on structural damage in coralline algae - in the field or in the lab. Such a study is beyond the scope of this paper. It is known that Mg concentration affects the Young's modulus of the skeletal tissues. To account for this we conducted a material property sensitivity test (page 11), which highlighted the fact that any changes in Mg concentration, due to environmental changes would not have an effect on the stress results, but strain will be affected.

With the current focus on the simulations alone, it would also be helpful to provide more information on the modelling itself. There is no information given on what is calculated (governing equations or concise citations). Thus, a reader interested in the topic but not familiar with the analysis is not well served.

To accommodate the suggestion we have amended the manuscript.

Page 4 line 81
FEA works by transforming a continuous structure into a discrete number of elements which are connected to each other via nodes. The combination of elements and the interconnecting nodes forms the mesh. Appropriate material properties (Young's modulus and Poisson's ratio) are assigned to the elements to mimic the elasticity of the structure. Adequate boundary conditions (magnitude and direction of loading and constraints) are applied and then nodal displacements are calculated in response to the applied boundary conditions and material properties of the model. The nodal displacement is used to calculate the strain and subsequently stress (using the Young's modulus, see equation 2) and hence mechanical performance of complex structures can be inferred. (For mathematical equations see Mathematics of FEA, (Rayfield, 2007) supplementary material)
E (Young's modulus) = σ (stress)/ ϵ (Strain) (2)

Comment 2 - Chris Evenhuis

An interesting choice has been made in the loadings. The loading is asymmetric as the forces are applied to the top-left corner over 40 µm *strips while the opposing forces are from the bottom-left is over a* 40 µm *strip on the side but the whole bottom surface. This results the loading being mostly compressive down the diagonal of the cube, but with some shear along the x axis. What is the ratio of the compressive to shear forces?*
Is this mixing of compressive and shear forces intentional? I would imagine that main impact on the structures from wave motion would be large scale shear stresses rather than compressive ones (the fractures in the picture are lateral which suggests they are more susceptible sheer forces). Similarly, I would anticipate that borers would also predominately exert shear stresses, just on a much smaller scale. It may be more instructive to change how the applied and constraint forces so that it better reflects the geometry of the natural environment. Maybe setting up two sets of loadings would be a good way to investigate the relative effects of shear and compressive loads.

The mixing of compressive and shear forces were done due to recreating the same loading environment as Ragazzola et al. (2012). As pressure is applied to the top left corner, there will be a mixture of both compressive stress as well as shear stress. Constraining the bottom surface of the cube and the right hand side, and having the load occurring in the top left hand corner, simulated the edge of the thallus receiving the load. Additionally, we are now including simulations distinguishing load types to include only shear and compressive loads instigated by the comments of the reviewer (see below).

Page 5 line 98
The loading and constraint taken from Ragazzola et al. (2012) were a mixture of shear and compressive forces, which simulated boring forces by an organism exerted on the exposed corner of an attached thallus. As it was assumed that these organisms were more prone to shear forces than compressive ones, we also assessed the effect of sole compressive or sole shear forces on the compartmentalised and the biologically realistic model.

Page 9 line 181
2.1.4. Comparison between shear and compressive loads
The biologically realistic and the compartmentalised model were exposed to different loading scenarios in Abaqus. This included the original load setup explained earlier in section 2.1.3 (Fig. 1a); the compressive loads, where the load was applied to the top of the cube opposite the constraint (Fig. 1b); and shear loads, where the load was applied on the face adjacent to the bottom constraint (Fig. 1c).

As this part of the study moved on from the initial research of Ragazzola et al. (2012), it was decided to use loads defined experimentally based on real wave velocities. Starko et al. (2015) used wave velocities of up to 3.5 $\mathrm{m\,s^{-1}}$ to assess the effect of branching in flexible wave swept macroalgae, in which they also measured the drag force. Water velocity experienced by subtidal marine macroalgae is on the order of magnitude of 1 $\mathrm{m\,s^{-1}}$ (Carrington, 1990).

Hence, we used a drag force (0.9N) corresponding to a wave velocity of 3.5 $m\,s^{-1}$ experienced by a heavily branched macroalgae (similar in branching to our rhodoliths) to carry out our load type comparison tests. Here we have kept the force per unit area constant in order to compare the compartmentalised model to the biologically realistic model. Strain energy is dependent on volume, therefore in order to compare the total strain energy between the models we had to take into account the difference in calcite volume between the biologically realistic and the compartmentalised model ~~(using equation 1)~~ (Dumont et al., 2009).

Page 10 line 197
Using these more environmentally significant forces, we can see that the stresses and strains exerted by these organisms were not as large as those taken from Ragazzola et al. (2012). Accounting for the change in units, the differences between the von Mises stress results are on the order of magnitude of 10^9 instead of 10^{11}.

In the biologically realistic model, under the original load setup, stress dissipated throughout the model from the corner where the load was applied to the constrained corner (Fig. 1a). While under the compressive load setup, the stress had a top to bottom distribution (from the loaded surface to the constrained surface) with a slight increase in stress surrounding the cavities in the model (Fig. 1b) and under the shear load setup, two thin bands of higher stress perpendicular to each other were observed (Fig. 1c). The average von Mises Stress, 95th percentile of (Mises) stress and total strain energy were slightly larger under the shear load setup compared to the compressive load setup (Table 1). All three values were larger than the compressive or shear model in the original load set up (Table 1).

In the compartmentalised model, under the original load setup the stress dissipated throughout the model from the corner where the load was applied to the constrained corner (Fig. 1d). While under the compressive load setup, the area of higher stress was restricted to the top of the model where the load was applied (Fig. 1e) and under the shear load setup, the area of high stress spread from the right hand side near the constrained corner (Fig. 1f). The average von Mises stress, 95^{th} percentile of (Mises) stress and the total strain energy were largest under sole shear loads and smallest in the compressive load model, with values for the original set up falling in between (Table 1).

Note the shear load in the compartmentalised model was applied differently to the arrangement for the biologically realistic model. As the compartmentalised model was not able to run under a sole shear load, like the biologically realistic model, a small constraint on the opposite face (1 µm) was added to help stabilise the model (Fig. 1f).

Page 15 line 281
Here we have demonstrated that the geometric models were more susceptible to shear loads than compressive loads, however the differences were minimal (Table 1). Similar differences between compressive and shear systems have been documented previously in another filamentous cellular material, wood. The fatigue properties of wood laminates were found to be an order of magnitude higher in compressive strength than shear strength (Bonfield and Ansell, 1991). This was also the case with nacre found in abalone shells, an organic-inorganic composite material made of mainly aragonite, which similarly had an order of magnitude difference between shear and compressive strength (Menig et al., 2000).

The compartmentalised model under sole shear or sole compressive loads was less accurate at representing the more biologically realistic model. This was seen in the stress distributions, which were only comparable between the biologically realistic and the compartmentalised models under the original load setup (Fig. 1). The compartmentalised model was especially inaccurate at representing the biologically realistic model under the shear load setup. The computed strain energies were too high for the model to run under a purely shear load and therefore an extra constraint was required to help stabilise the compartmentalised model (Fig. 1f). The regular cells in the compartmentalised model stabilised the model under the compressive load setup, whereas under a shear load setup the individual cells could not help stabilise the model in the direction of the shear load. This highlights the importance of natural variability in the biologically realistic model, which was missing from the regular compartmentalised model making it more susceptible to shear loads.

Interestingly, for the biologically realistic model, the largest results occurred under the original load (a combination of both shear and compressive loads), whereas for the compartmentalised model the largest results occurred under the shear load. This finding highlights the susceptibility the compartmentalised model had to shear loads compared to the biologically realistic model. However it is important to note that the forces used were derived based on experiments on flexible macroalgae found in the wave-swept intertidal zone. Rhodoliths are made up of high Mg-Calcite and are found unattached on the bed. Hence they will experiences different drag forces compared to flexible attached wave swept macroalgae at similar velocities.

The values given in section 2.1 dont add up and the geometry specification is confusing. This is partly due to the Ragazzola paper, but the models need to be clearly specified. Ive attached a figure with best that I could make of the model by examining the figures. Also it needs to be cleared noted that the in the y direction each layer has the same thickness (i.e. the top and bottom surface has the same thickness as the inner ones) but in the x direction the sides (left most and right most walls) have half the thickness of the inner ones. That is, the model is not translations of a unit cells.

The model dimensions are the same as in the Ragazzola paper to enable effective comparison. The measurements used by the reviewer to recreate the model are different from the measurements stated in our paper and hence that is why the reviewer's dimensions do not add up to our total. We have rechecked our figures and taking into account rounding (as Abaqus can

only measure to 2 decimal places) they do add up. The authors suggest the following changes to the manuscript to avoid any open questions which might lead to this kind of misunderstanding.

Page 6 Line 114
The inter-wall thickness was the thickness of a single cell wall in the x direction (between filaments). Therefore the internal walls of the model had two inter cell walls, whereas the external walls (the left outermost and right outermost) only had one inter cell wall each. The intra-cell thickness was the cell wall thickness between cells in the y-direction. As the rhodolith grows as a set of filaments, there was only one cell wall between two cells in the y-direction (Fig. 2).

Graphing the results makes assessment much easier. Ive done a quick plot of the data as an example. Is there any different between 2D and 2D 422 µ*atm results and the 3D compartment and 3D compartment 422* µ*atm results? Other than a change in the 5 sig fig for the strain, these two sets of results appear identical and there is no difference between the values and nothing in the text to indicate that these are distinct results. This should be removed from the table.*

There is no difference in the results; they are the same, but to make it easier to understand the table we duplicated entries. We understand the reviewer's comments, however we believe the graph makes the information harder to understand and hence we have kept the table.

After the effort was made to create a 3D model of the actual skeleton, it would be good to have some information about the geometry of the skeleton. It is hard to judge from ~~figure 6~~, but it would appear that the skeleton has a structure more like Swiss cheese than a regular lattice.

The authors acknowledge the reviewer's comments about the geometry of the biological model. Please find below our additions to the manuscript.

Page 7 Line 133
This cube was selected at random within the scan of the rhodolith (Fig. 3 a-d), as using the CT scan the summer winter layers could not be distinguished.

Page 10 line 201
Comparison of the internal morphology between the compartmentalised model and the biologically realistic model showed similarities. Both models had regularly distributed cavities. However unlike the compartmentalised model the biological model cavities were spheroidal and, due to the natural variation within these specimens, the arrangement of cavities was not as regimented as in the compartmentalised model (Fig. 4). Both the biologically realistic and the compartmentalised model had the same percentage volumes of calcite and cavities whereas the corridor model had a lower percentage volume of calcite (Table 2).

Page 12 line 224
The importance of these structures is highlighted by the geometric model with compartments (the compartment model) being the most stable of the geometric structures assessed and also most comparable - in terms of percentage volume of calcite, stress distribution and magnitudes of average stress and total strain energy - to the biologically realistic model. This highlights the importance of geometry changes, which our method accurately captured, to the distribution and magnitude of stress.

Should the total strains for each model be compared to the same total stress and the data interpreted as a linear section of a stress-strain curve? Can the results be interpreted in terms of changes in brittleness? How we sure that the data is on the linear part of the curve? For example, maybe the stresses in the perturbative regime? What would happen if the applied force is varied? I imagine that the geometry dictates the stress strain relationship. Can the models be run with increasing loadings until a fracture occurs, or is this beyond the capability of the software?

The analysis used here employs a linear elastic model, so stress and strain will vary in a linear fashion as dictated by the Young's modulus. Loads can be increased until values that would induce fracture are reached but the overall pattern of stress and strain will remain the same, as will the relative differences between the models with varying geometry. As our aim here is to compare the relative performance of different model types, we have elected not to present a series of further analyses with varying loads. Furthermore, the fracture properties for coralline algae are not well understood and fracture stress and strain is unknown. Further experimental work is required to obtain accurate fracture properties.

Assuming that all the results lie on the linear section a stress-strain curve, can it concluded that the biological model has a different bulk modulus of elasticity. Even if this holds the modulus of elasticity isn't that relevant to the fracture process, which I would guess is the more relevant quantity. The von Mises is a measure of local stress, and therefore has a distribution across the model. In a fracturing process the extremes of the distribution are important, not the average of the distribution. I think it would be good to include in the table something like the 90^{th} *or* 95^{th} *percentile of the von Mises stresses.*

As these models are representing the same organism, with similar volumes, it is assumed that the elastic modulus is the same. Hence this study is effectively analysing the effect of shape on the structural integrity.

The reviewer makes a valid point; indeed in the fracturing process the extremes of the distribution are important. Hence we have added the 95^{th} percentile for the three comparison models (the 3D corridor, 3D compartmentalised and the biologically realistic model to our main table (Table 3).

Page 8 Line 167
The 95^{th} percentile of (Mises) stress was additionally used as a comparison between the 3D corridor, compartmentalised and biologically realistic model as this metric highlighted the extremes of the von Mises Stress distribution - an important parameter to highlight fracture potential.

Page 10 Line 201
This was also seen with the 95^{th} percentile of (Mises) stress which showed the compartmentalised and the biologically realistic model result in similar values. Whereas the corridor model resulted in both the 95^{th} percentile of (Mises) stress and the strain energy an order of magnitude higher, while the average stress was over double the amount than both the compartmentalised and biologically realistic model (Table 3).

Also, rather than plotting the stresses over the entire 3D model (which shows only the surface stresses) could the areas experiencing the highest stresses be identified? For example, the compartment might have a maximum on in the middle of the left facing surface while the biological model might have a maximum in the middle of the right facing surface. Similarly, the most informative part of the 3D stress might be a slice through the centre. The plots in paper show the stresses on the surface which are affect by the conditions - I would expect these surface layer stress to most sensitive to simulation details like size of model, while the central ones would be more stable. On the other hand, a fracture probably starts at the surface and propagates inwards, in which case the surface stresses are most relevant.

As the surface layers are directly in contact with the loads and the constraints this is where the model is most sensitive, hence why the minimum and maximum stresses were located on the surface (Fig. 5). The minimum and maximum values, therefore, do not provide much more information than already provided by the surface plots and hence are not discussed further. We checked, and the stress distribution does not change throughout the model hence we have chosen not to figure this further in the revised manuscript.

Page 8 Line 160
Stress results were also displayed as scaled colour plots. Stress distribution throughout the model was very similar to surface stress distribution. The surfaces of the model were more sensitive to the loads and constraints, due to immediate contact with the boundary conditions. The minimum and maximum von Mises stress values were found on the surfaces of the models, being more influenced by the position of the boundary conditions and complexities in the geometry. Hence, the minimum and maximum values did not provide any additional information on the overall structural integrity of the model than that provided by the surface contour plots.

What is the relationship between in the von Mises stress and the total stress? Do the von Mises stress integrate up to the total stress? Would this total stress be the force over the area of the skeleton in contact with the boundary , or would it be bulk area?

Von Mises stress, a function of each of the principle stresses which represent compressive or tensile stress, is a parameter used to determine failure i.e. if the maximum value of von Mises stress induced in the material is greater than the failure stress of the material the design will fail. However we are not using the parameter to determine failure but to compare relative stress between different structures. So here von Mises stress is the total stress and the total stress is the force over the bulk area.

If the model is converged with respect to mesh points the results wont depend on the number of elements - that is, it doesnt matter whether a triangular, hexagonal, random etc. mesh is used the answer should be same. Comparing the results for 3D corridor with a hexagonal mesh (1×106 *elements) with the tetrahedral mesh (*2×106*) the total strain differs by an order of magnitude. This indicates that one (or more likely both) of these models is far from convergence. What checks of convergence has been done? Without being sure that the results are converged how is it possible to compare the results of one geometry to another?*

A convergence test was performed on both meshes, where the mesh size was subsequently decreased until the average von Mises stress became constant. We now include these analyses in the paper. Theoretically the different type of elements, once converged, should not have an impact on the distribution of the stress. However in reality the stiffness of the tetrahedral mesh, with better interlocking elements, does affect the results. Please see below for our addition to the manuscript.

Page 7 line 145
Convergence test were performed for each mesh type in order to determine the minimum mesh size required. The mesh size was decreased until the average von Mises value no longer changed relative to mesh size. Hypothetically, all refined meshes should converge to similar results yet our converged von Mises stress value was an order of magnitude different between the hexagonal and tetrahedral mesh. This was due to the shape of the tetrahedral elements and the way tetrahedral elements interlock together, making a tetrahedral model stiffer than a hexagonal model. This is reiterated by Dumont et al. (2005), who found that comparing a converged 4-node linear and a stiffer 10-node quadrilateral tetrahedral mesh of the same model gave different mean stress values, but within 10%. In order to compare the 2D to 3D geometric models, the corridor model was meshed with 4- node linear hexagonal elements. As tetrahedral elements were better at capturing the complex geometry of the biological model, all models were then meshed with 4-node linear tetrahedral elements in order to be compared to the biologically realistic model and to each other.

Related to the last point, no uncertainties given. A simple assessment of the variation of the results with change in cell size parameters or number of grid points a rough indication of variations.

In response to the first point, we now provide results that indicate how sensitive the model is to changes in material properties.

Varying cell size parameters represents a substantial amount of work and is beyond the scope of this paper but is certainly something to follow up in future work. However care was taken in choosing the cell sizes used in the study. A significant number of cells were measured under SEM in both current and year 2050 conditions and the average measurements were used to create the model geometries here.

It is not clear what the reviewer means by number of grid points and therefore we are not able to respond.

Page 9 line 181
To analyse how sensitive the models were to changing material properties, a set of 2D and 3D corridor models with different Young's modulus (maximum and minimum Young's modulus values of two different bivalves - *Mytilus edulis* and *M. californianus*) were analysed.

Page 14 line 280
However it is important to note that the sensitivity test highlighted that increasing the Young's modulus by 120% did not result in any change in stress, as the stress is directly proportional to force and inversely proportional to area (Table 4). Whereas, as strain is inversely proportional to Young's Modulus (equation 2), increasing the Young's modulus caused a decrease in the maximum and minimum strain values - as seen in other studies on organisms such as macaques (Strait et al., 2005), alligators (Reed et al., 2011) and pig skulls (Bright and Rayfield, 2011). Although structures with heterogeneous material (in this case seasonality affecting Mg concentrations) did display differences in both stress and strain (Reed et al., 2011; Strait et al., 2005).

References

Andersen, L. and Jones, C.: Coupled boundary and finite element analysis of vibration from railway tunnels - a comparison of two-and three-dimensional models, Journal of Sound and Vibration, 293, 611-625, 2006.

Bonfield, P. and Ansell, M. P.: Fatigue properties of wood in tension, compression and shear, Journal of Materials Science, 26, 4765-4773, 1991.

Bright, J. A. and Rayfield, E. J.: Sensitivity and ex vivo validation of finite element models of the domestic pig cranium, Journal of Anatomy, 219, 456-471, 2011.

Carrington, E.: Drag and dislodgment of an intertidal macroalga: consequences of morphological variation in Mastocarpus papillatus Ktzing, Journal of Experimental Marine Biology and Ecology, 139, 185-200, 1990.

Denny, M. W., Miller, L. P., Stokes, M. D., Hunt, L. J. H., and Helmuth, B. S. T.: Extreme Water Velocities: Topographical Amplification of Wave-Induced Flow in the Surf Zone of Rocky Shores, Limnology and Oceanography, 48, 1-8, 2003.

Dudgeon, S. R. and Johnson, A. S.: Thick vs. thin: thallus morphology and tissue mechanics influence differential drag and dislodgement of two co-dominant seaweeds, Journal of Experimental Marine Biology and Ecology, 165, 23-43, 1992.

Dumont, E., Grosse, I., and Slater, G.: Requirements for comparing the performance of finite element models of biological structures, Journal of Theoretical Biology, 256, 96-103, 2009.

Dumont, E. R., Piccirillo, J., and Grosse, I. R.: Finite-element analysis of biting behavior and bone stress in the facial skeletons of bats, The Anatomical Record Part A: Discoveries in Molecular, Cellular, and Evolutionary Biology, 283A, 319-330, 2005.

Gaylord, B., Blanchette, C. A., and Denny, M. W.: Mechanical Consequences of Size in Wave-Swept Algae, Ecological Monographs, 64, 287-313, 1994.

Menig, R., Meyers, M. H., Meyers, M. A., and Vecchio, K. S.: Quasi-static and dynamic mechanical response of Haliotis rufescens (abalone) shells, Acta Materialia, 48, 2383-2398, 2000.

Ragazzola, F., Foster, L. C., Form, A., Anderson, P. S. L., Hansteen, T. H., and Fietzke, J.: Ocean acidification weakens the structural integrity of coralline algae, Global Change Biology, 18, 2804-2812, 2012.

Rayfield, E. J.: Finite element analysis and understanding the biomechanics and evolution of living and fossil organisms, Annu. Rev. Earth Planet. Sci., 35, 541-576, 2007.

Reed, D. A., Porro, L. B., Iriarte-Diaz, J., Lemberg, J. B., Holliday, C. M., Anapol, F., and Ross, C. F.: The impact of bone and suture material properties on mandibular function in Alligator mississippiensis: testing theoretical phenotypes with finite element analysis, Journal of Anatomy, 218, 59-74, 2011.

Romeed, S., Fok, S., and Wilson, N.: A comparison of 2D and 3D finite element analysis of a restored tooth, Journal of oral rehabilitation, 33, 209-215, 2006.

Starko, S., Claman, B. Z., and Martone, P. T.: Biomechanical consequences of branching in flexible wave-swept macroalgae, New Phytologist, 206, 133-140, 2015.

Strait, D. S., Wang, Q., Dechow, P. C., Ross, C. F., Richmond, B. G., Spencer, M. A., and Patel, B. A.: Modeling elastic properties in finiteelement analysis: How much precision is needed to produce an accurate model?, The Anatomical Record Part A: Discoveries in Molecular, Cellular, and Evolutionary Biology, 283, 275-287, 2005.

Table 1: Average von Mises Stress, 95^{th} percentile of (Mises) stress and total strain energy for the different load types exerted on the biologically realistic, compartmentalised and corridor model. Total strain energy for the biologically realistic model has been corrected for calcite volume ~~(equation 1)~~. The compartmentalised model under the shear loading type is highlighted in grey to reiterate that the loading setup is different to the biologically realistic model under a shear loading type.

Model	Loading Type	Average von Mises Stress (N µm^{-2})	95^{th} Percentile of (Mises) Stress (N µm^{-2})	Total Strain Energy (J)
Biologically realistic				
	Compressive	2.34E-04	4.08E-04	2.99E+05
	Shear	2.83E-04	6.07E-04	5.47E+05
	Original (Shear + Compressive)	3.49E-04	7.21E-04	8.71E+05
Compartmentalised				
	Compressive	2.42E-04	2.96E-04	2.34E+05
	Shear	4.27E-04	1.03E-03	1.63E+06
	Original (Shear + Compressive)	4.10E-04	8.25E-04	9.63E+05

⋆ Strain energy corrected for calcite volume

Table 2: Percentage volumes of calcite and cavities in the biologically realistic model, the corridor and the compartmentalised model.

Material	Biologically Realistic Model	3D Corridor	3D Compartmentalised
Volume of Calcite (μm^3)	3.09E+05	1.94E+05	2.87E+05
Volume of Cavities (μm^3)	1.83E+05	2.60E+05	1.67E+05
Percentage of Calcite	63%	43%	63%
Percentage of Cavities	37%	57%	37%

Table 3: Mesh type, number of elements, average von Mises stress, 95^{th} percentile of (Mises) Stress and total strain energy for the different models.

Model	Mesh Type	Number of Elements	Average von Mises Stress (Pa)	95^{th} Percentile of (Mises) Stress (Pa)	Total Strain Energy (J)
422 µatm 2D model	Quad	16368	1.67E+11		8.91E+08
589 µatm 2D model	Quad	1889	5.17E+11		1.27E+10
3D Corridor	hexagonal	202304	1.72E+11		1.11E+11
3D Corridor $\star$	hexagonal	202304			4.79E+11
3D Corridor (model 1)	tetrahedral	2125549	7.46E+10	2.21E+11	1.75E+10
422 µatm Compartmentalised (model 2)	tetrahedral	3442433	2.75E+10	5.36E+10	4.28E+09
Biologically realistic model (model 3)	tetrahedral	2106858	2.74E+10	5.63E+10	5.21E+09
589 µatm Compartmentalised (model 4)	tetrahedral	1707673	4.98E+10		8.81E+09

Table 4: Average von Mises Stress and total strain energy for the comparison of the different material properties in the 2D and 3D corridor models.

Material	Young's Modulus (Pa)	Average von Mises Stress (Pa)	Total Strain Energy (J)
2D			
Calcite	3.60E+10	1.67E+11	8.91E+08
M. edulis -min	4.39E+10	1.67E+11	7.30E+08
M. californianus -min	4.79E+10	1.67E+11	6.69E+08
M. edulis -max	7.18E+10	1.67E+11	4.47E+08
M. californianus -max	7.93E+10	1.67E+11	4.04E+08
Material	Young's Modulus (Pa)	Average von Mises Stress (Pa)	Total Strain Energy (J)
3D Corridor			
Calcite	3.60E+10	7.46E+10	1.75E+10
M. edulis -min	4.39E+10	7.46E+10	1.43E+10
M. californianus -min	4.79E+10	7.46E+10	1.31E+10
M. edulis -max	7.18E+10	7.46E+10	8.77E+09
M. californianus -max	7.93E+10	7.46E+10	7.94E+09

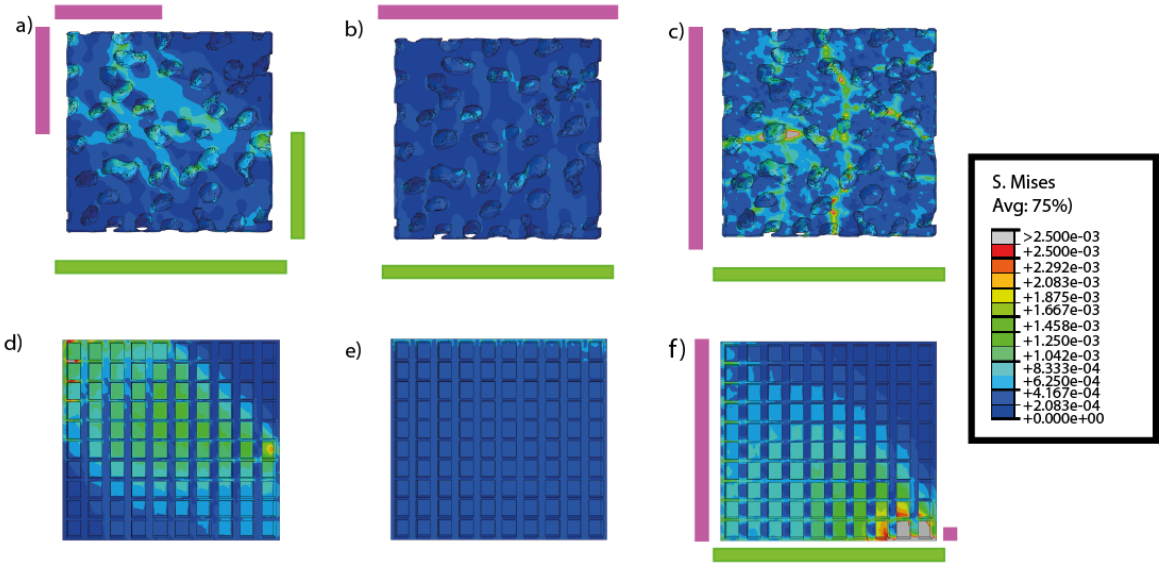

Figure 1: The von Mises Stress patterns on the biologically realistic model (a, b & c) and the compartmentalised model (d, e & f) in different loading situations; the original (mixture of both shear and compressive loads) (a & d); compressive load (b & e) and the shear load (c & f). The different load situations (pink box) are shown on the biologically realistic model as well as the constraints (green boxes). The shear load for the compartmentalised model was set up slightly differently and hence the loading setup is displayed on the model. Units= N μm^{-2}

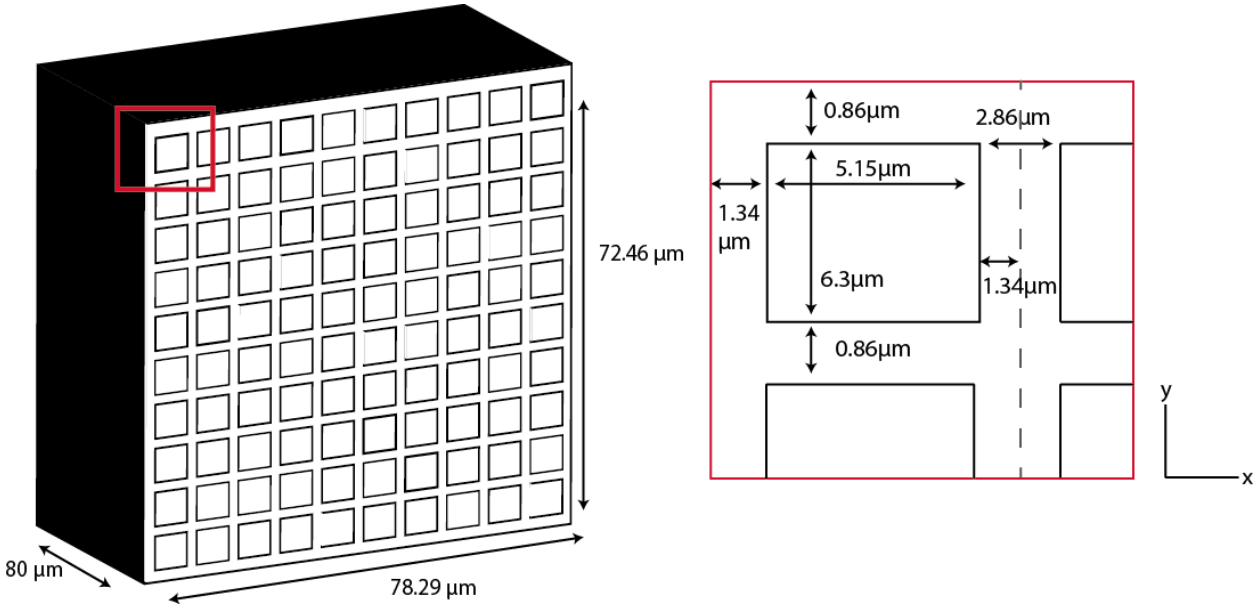

Figure 2: Dimensions used in the 3D corridor model. Units $=\mu$m

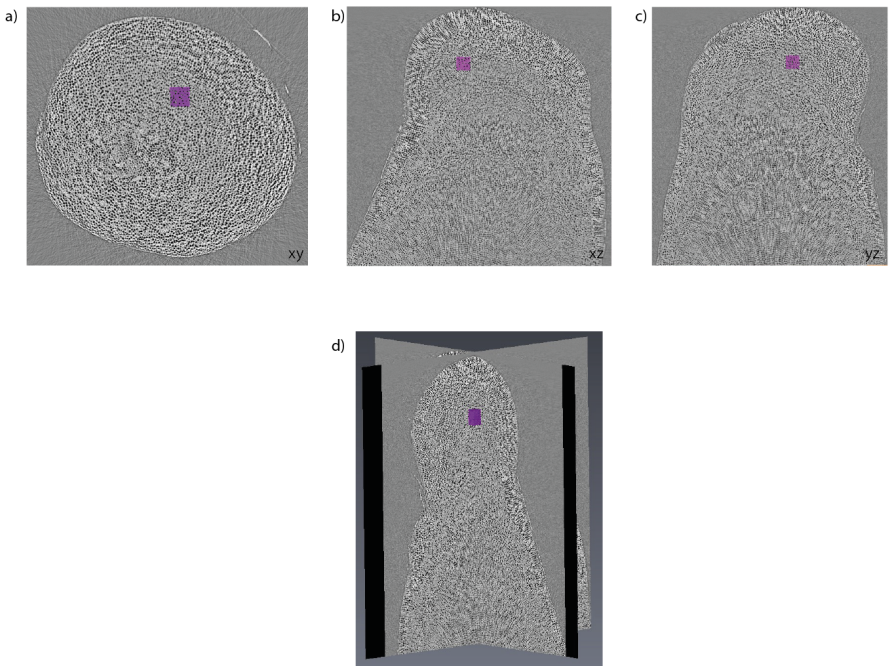

Figure 3: Orthoslice projections in the different planes of a rhodolith thallus: a) xy direction; b) xz direction; c) yz direction and d) in 3D format. The purple box highlights where the 80μm x 80μm cube was selected

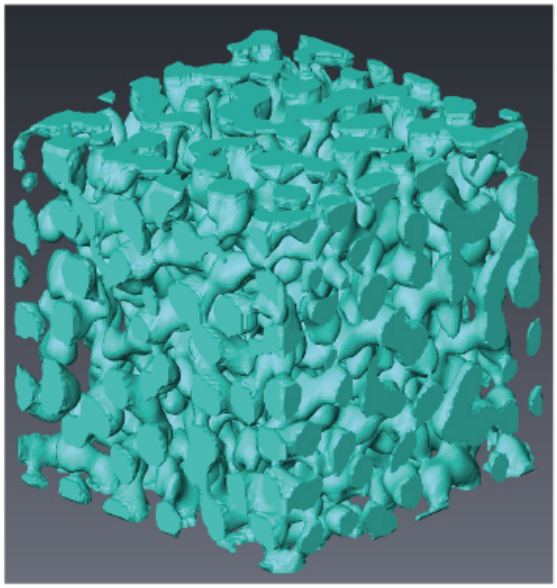

Figure 4: The inside spheroidal cavities of the biologically realistic cube

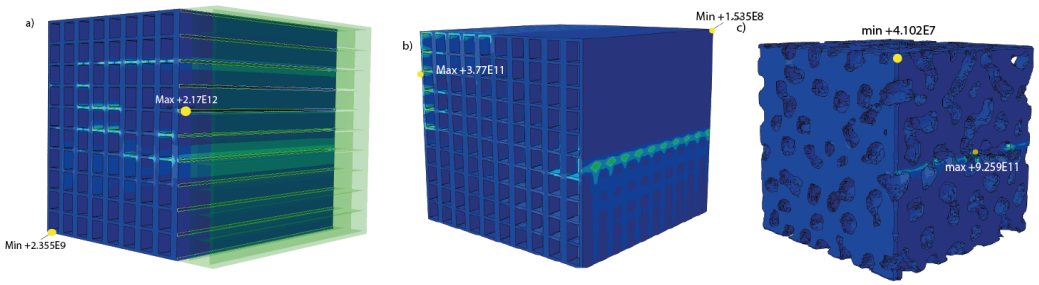

Figure 5: The minimum and maximum von Mises stress values of a) the corridor model, b) the compartmentalised model and c) biologically realistic model. Units = Pa.